Bulletin of the Seismological Society of America, Vol. 94, No. 5, pp. 1579–1594, October 2004

Quantifying Sensitivities of PSHA for France to Earthquake Catalog Uncertainties, Truncation of Ground-Motion Variability, and Magnitude Limits

by Celine Beauval* and Oona Scotti

Abstract The results of this study clearly identify four key parameters controlling the estimation of probabilistic seismic hazard assessment (PSHA) in France in the framework of the Cornell–McGuire method. Results in terms of peak ground acceleration demonstrate the equally high impact, at all return periods, of the choice of truncation of the predicted ground-motion distribution (at $+2\sigma$) and of the choice between two different magnitude-intensity correlations. The choice of minimum magnitude (3.5/4.5) on hazard estimates can have an important impact at small return periods (<1000 years), whereas the maximum magnitude (6.5/7.0), on the other hand, is not a key parameter even at large return periods (10,000 years). This hierarchy of impacts is maintained at lower frequencies down to 5 Hz. Below 5 Hz, the choice of the maximum magnitude has a much greater impact, whereas the impact due to the choice of the minimum magnitude disappears. Moreover, variability due to catalog uncertainties is also quantified; these uncertainties that underly all hazard results can engender as high a variability as the controlling parameters. Parameter impacts, calculated at the centers of each source zone, show a linear trend with the seismicity models of the zone, demonstrating the lack of contributions coming from neighboring zones. Indeed, the region of influence that contributes to the PSHA estimate at a given site decreases with increasing return periods. The resulting overall variability in hazard estimates due to input uncertainties is quantified through a logic tree, obtained coefficients of variation vary between 10% and 20%. Until better physical models are obtained, the uncertainty on hazard estimates may be reduced by working on an appropriate magnitude-intensity correlation.

Introduction

If many studies exist in the literature on applications of probabilistic seismic hazard assessment (PSHA) and ever more sophisticated approaches, there are insufficient studies that deal with the fundamental mechanics and sensitivities of PSHA. Sensitivity studies are often limited to studies focused on predominantly two inputs: the seismotectonic zoning and the ground-motion attenuation relationship. Little effort is put into understanding the mechanics of the probabilistic computations, on clearly stating the parameters chosen, and in quantifying the impact of such parameters on the final results. Consequently, results are very difficult to compare from one study to the next and the source of the differences is not easy to understand. However, probabilistic seismic hazard estimation is the basis for the establishment of seismic hazard maps and application of earthquake-resistant building regulations. It is fundamental to understand its mechanics thoroughly to not only clearly define its limitations and uncertainties but also to propose new research to reduce the uncertainty. This study is an attempt to go in that direction.

PSHA requires inputs and models that can carry great uncertainties. These uncertainties and their impacts on hazard results depend on the region of interest. This study concerns the French metropolitan area; the objective is to quantify the impact on hazard estimations due to the choice of key parameters that are required by the probabilistic method of Cornell–McGuire (Cornell, 1968; McGuire, 1976). The majority of existing sensitivity studies in PSHA deal with the impact of the zoning, either considering different zoning or using soft boundaries (Bender and Perkins, 1993), as well as with the impact of the attenuation relationship used (calculating hazard with different available attenuation relationships). In this study, we build on previous efforts and con-

*Present address: Institute of Geosciences, University of Potsdam, PF 601553, D-14415 Potsdam, Germany.

sider a single seismotectonic zoning and a single attenuation relationship. The reference seismotectonic zoning was elaborated by the AFPS-EPAS working group (working group of the French Association for Earthquake Engineering–Probabilistic Estimation of Seismic Hazard), composed of several experts from various fields: geology, geophysics, seismology, engineering (Autran *et al.*, 1998). The attenuation relationship used in this study was derived from a primarily European database (Berge-Thierry *et al.*, 2003) and is now the reference attenuation relationship for France in deterministic hazard studies. Previously, several relationships had been used in PSHA studies in France (e.g., by Dominique *et al.*, 1998), such as Mohammadioun and Pecker (1993), Tento *et al.* (1992), Ambraseys (1995), and Ambraseys *et al.* (1996).

The remaining uncertainties explored in this article include catalog uncertainties concerning the magnitude and location determinations, the magnitude-intensity (M-I) correlation used to compute historical magnitudes, the truncation of the ground-motion probability density function, the minimum magnitude contributing to the hazard, and the maximum magnitudes that could occur in the source zones. Considering the large scatter of most attenuation relationships (Douglas, 2003), PSHA must take into account the lognormal distribution. However, few studies address the problem of truncation of this distribution, although the consequences of no truncation both at small and large return periods had been evoked a long time ago (Reiter, 1990; Bender and Perkins, 1993). Similarly, very few sensitivity studies consider the choice of the minimum magnitude used in the PSHA calculations. The influence of this parameter on hazard estimation is not new (Benjamin and Associates, 1989; Reiter, 1990) and is tightly linked to the way the scatter of the attenuation relationship is taken into account. In this article, the impact of the choice of the minimum magnitude is quantified for the French territory. At the other end of the magnitude range, the choice of the maximum magnitudes of the source zones, which is often addressed in PSHA sensitivity studies (Giner *et al.*, 2002; Rebez and Slejko, 2000), is also considered here.

In this study, hazard is computed at the centers of 17 selected source zones of the AFPS-EPAS zoning. We consider that these source zones contain a sufficient number of seismic events to estimate the recurrence parameters required by the probabilistic method. Concentrating only on 17 sites, we do not need to use maps and, thus, representing variability results is easier; individual impacts of parameters can be compared between geographical sites and also between different return periods. Moreover, we show that impacts are related to the seismic characteristics of the source zones, leading to a better understanding of impact variability from one zone to another.

The uncertainties in magnitude and location of earthquakes are explored through the generation of synthetic catalogs. To estimate individual parameter impacts, on the other hand, a reference set of parameters is first defined and parameters are modified one at a time. The percentage change due to each individual parameter variation is quantified. Reference and alternative values are carefully chosen to describe the most representative interval of possible values. Finally, the frequency dependence of the parameter impacts on hazard estimates is also computed.

Choice of Probabilistic Methodology

The following is a concise summary of the Cornell–McGuire approach for probabilistic seismic hazard assessment (Cornell, 1968; McGuire, 1976).

The probabilistic estimation of seismic hazard at a site consists in computing the annual rate of occurrence of a ground-motion parameter exceeding a specified level (hereafter called the target level, A_T). The most common ground-motion parameter used in this study is the peak spectral acceleration. The annual rates of interest in hazard assessment range from 0.01 to 10^{-7} (and even 10^{-8}; e.g., in the PEGASOS project [Bommer *et al.*, 2004]); but it is common to refer to the inverse of the annual rate, the return period (100 to 10^7 years), although it is a term that generates confusion. It is important to recall that earthquake occurrences are not assumed to be periodic but Poissonian. The annual rates of several target levels A_T are computed, so that for any return period of interest the corresponding acceleration is deduced by interpolation.

The Cornell–McGuire method for the computation of rates of exceedance relies on four steps:

1. The sources of seismicity must be identified; these sources are faults in regions where active faults can be delineated clearly (highly seismic regions) and areas in regions where active faults are poorly known. Limits of areas are drawn according to geological, geophysical, or seismological homogeneous features. France shows diffuse intraplate seismicity; hence, only source zones can be used. The zoning we use (Autran *et al.*, 1998) proposes 39 zones for France and its frontiers along with an estimation of the average depth of earthquakes for each source zone. Our study will focus only on the 17 most seismically active zones (Fig. 1).
2. Inside each source zone, the magnitude range of possible earthquakes and their corresponding annual rates of occurrence must be estimated. The truncated exponential Gutenberg–Richter model (e.g., Kramer [1996]) is used here. The seismic parameters (slope of the Gutenberg–Richter and the seismic rate) are calculated from the data, and a maximum magnitude is attributed to the source zone.
3. An attenuation relationship is used to predict the acceleration engendered at the site by a seismic event of magnitude M located at the distance R from the site. The Berge-Thierry *et al.* (2003) attenuation relationship is used here. For each couple (M,R), the relationship yields

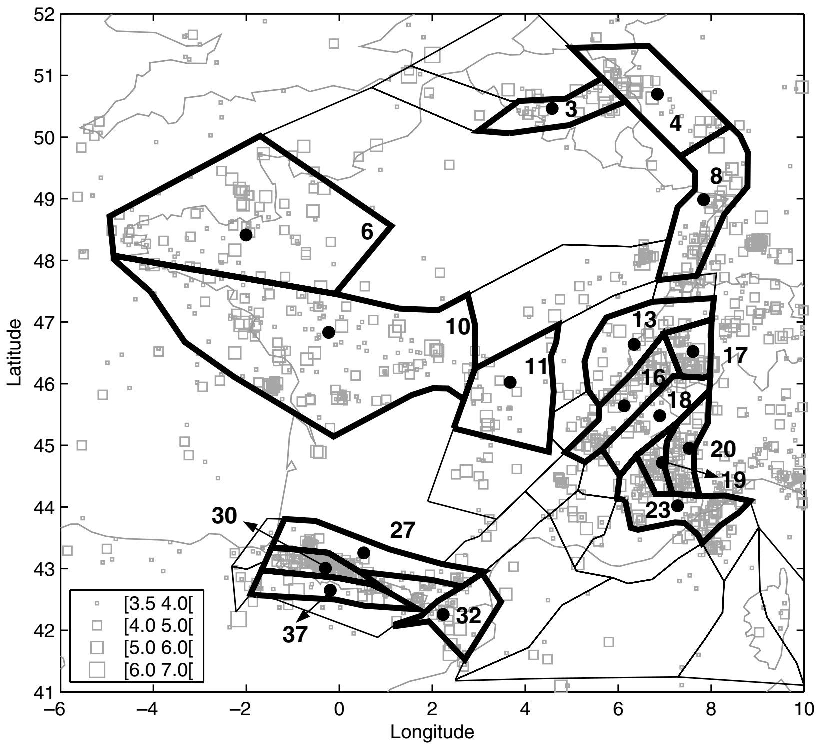

Figure 1. French seismic catalog in the period 1356–1999. Dark lines, AFPS-EPAS seismotectonic zoning; thick dark lines, selected source zones (with index of source zones and sites).

a normal probability density function (PDF) for logarithms of accelerations, with mean value,

$$\log_{10}(A) = aM - \log_{10}R + bR + c, \qquad (1)$$

and standard deviation σ. R is the hypocentral distance. The numerical values corresponding to the peak ground acceleration (PGA, accelerations at 34 Hz) are $a = 0.3118$, $b = -9.303\text{e} - 4$, $c = 1.537$, and $\sigma = 0.2923$, for rock sites. This distribution is used to calculate the probability for the couple (*M,R*) to engender an acceleration exceeding the target A_T, integrating the normal distribution from $\log_{10}(A_T)$ to $+\infty$, or to a multiple of σ when truncation is performed.

4. Finally, exceedance rates of all the existing couples (*M,R*) are summed.

In this study, annual rates are calculated for 80 accelerations between 30 and 3000 gal. Accelerations are then interpolated for return periods 100, 475, 10^3, 10^4, and 10^5 years. Traditionally, 475 years is used for conventional buildings, whereas the return periods considered for nuclear safety can range from 10^3 to 10^7. Assuming that acceleration occurrences follow a Poissonian distribution, the annual rates λ are derived from the formula:

$$P = 1 - \exp(-\lambda t), \qquad (2)$$

where P is the probability of the occurrence of at least one acceleration higher than the target level over the time interval t. Thus, a return period of 475 years corresponds to the probability of 0.1 of exceeding at least once the acceleration level over 50 years.

The Fortran code used is an adapted version of CRISIS 2000 written by M. Ordaz (http://www.ifjf.uib.no/seismo/software/seisan/seisan.html). The main features of the initial code have been retained, only the subroutines dealing with the attenuation relationship have been modified and the deaggregation has been added.

Constructing the Catalog

The seismicity contained in the geographical window [−6°, 10°] in longitude and (41°; 52°) in latitude is considered (Fig. 1). The seismic catalog contains both instrumental and historical data. The homogeneous measure of earthquake size is the local magnitude M_L. The instrumental part of the catalog is provided by the Laboratoire de Détection Géophysique (LDG; Nicolas *et al.* [1998]) and covers the period 1962–1999. The historical part of the catalog covers the period 1500–1961 and is extracted from the SisFrance database that gathers events from the past 1000 years (SisFrance2000, www.sisfrance.net). For the purpose of this study, we estimated magnitudes only for events that are described by at least three intensity classes (intensity III or above; half degrees are used). For each event, average epicentral distances are computed for each intensity class based on assumed epicentral coordinates, given in the SisFrance database, and on all available individual observations. The poor-quality observations or those affected by site effects were not considered. Then, using the magnitude-intensity correlation, a magnitude for each intensity class is computed and the mean magnitude of all available intensity classes is then considered as the final magnitude for the event.

At the moment two M-I correlations are available. The coefficients of these M-I correlations are derived by regression. The difference between the two correlations comes from the selection of events chosen for calibrating the M-I conversions. In the first correlation all events having both an instrumental magnitude and macroseismic intensity observation are considered (Levret *et al.*, 1994):

$$M = 0.44 * I + 1.48 * \log_{10} Rh + 0.48, \qquad (3)$$

where M is the magnitude, I is the intensity, and Rh is the hypocentral distance (with all depths fixed at 10 km for simplicity). Magnitudes estimated with this correlation match the instrumental ones around 4–5, but the magnitude of stronger events is underestimated (see Levret *et al.* [1994], figure 13, p. 33). To match the few known strong instrumental events, a new correlation was established by Griot-Pommera and Scotti (2001) using only a subset of the best-documented events for the calibration. The corresponding coefficients are the following:

$$M = 0.64 * I + 1.86 * \log_{10} Re - 0.45, \qquad (4)$$

where Re is the epicentral distance. This second correlation leads to conservative estimates of maximum magnitudes. Therefore, the two available catalogs have the instrumental part in common, but they have different historical magnitudes. To compute annual rates, it is necessary to estimate the periods of completeness adapted to each catalog. For each interval of magnitude, the period of completeness is the time window in which the magnitudes are considered to be exhaustively and homogeneously reported (Table 1). There is an uncertainty about the determination of these time windows; this uncertainty is highest for magnitudes greater than 6.0 (very few events). The periods of completeness of this study rely on the Stepp's (1972) technique and a "linear" method, for which seismic rate is assumed to be constant and independent of time. In the linear method, cumulative numbers of events versus time are plotted for each magnitude interval and the last linear trend, which usually has the highest slope, is selected. These methods require large data sets, which may be available at a regional scale in the Alps and the Pyrenees, but not everywhere else. Therefore, periods of completeness were only determined for the entire catalog contained in the geographical window of Figure 1. Moreover, a recent study by Beauval and Scotti (2003a) showed that calculating the Gutenberg–Richter parameters, including magnitudes lower than 3.5, yields anomalously high b-values in the eastern parts of France. Building on the conclusions of that earlier article, we compute the seismic parameters on magnitudes 3.5 and greater.

Selecting the Seismic Source Zones and Computing Seismicity Models

Subcatalogs are extracted for each source zone of the seismotectonic zoning scheme (Autran *et al.*, 1998). The slope of recurrence curves (the b-value or β-value) and seismicity rate are calculated using Weichert's (1980) method. This method is a generalization of the likelihood methods of Aki (1965), Utsu (1966), and Page (1968). It is able to handle annual rates estimated on different periods of time. The β-value is chosen such that it maximizes the product of the probabilities of having observed each annual seismic rate. Estimated β-values depend less than least-square methods on the few events that make up the high-magnitude intervals. For all zones, the magnitude range used is [3.5 $M_{\max}^{\text{observed}}$]. Magnitudes are binned into 0.5 large magnitude intervals and used only within their completeness period. Such a width is chosen to ensure a minimum number of events inside each bin, but our tests have shown that reducing the width does not affect the results.

Because of the scarcity of data, seismic parameters can be estimated reliably in only 17 of the 39 source zones of the AFPS-EPAS zoning (Fig. 1 and Table 2). For these 17 zones, the number of events used varies between 14 and 183 (see Beauval [2003]). The standard deviation of β, as calculated by Weichert, is between 0.12 and 0.4. In the remaining 22 source zones, 15 have less than 10 events and 7 concentrate all the magnitudes in the magnitude bin [3.5–4.0]. The standard deviation of β in these rejected source zones is larger than 0.4 and the seismic parameters are therefore considered to be unreliable.

Probabilistic Computations and Quantification of Impacts

The hazard and the uncertainties are estimated in this study only at the centers of the 17 source zones (coordinates of "centers" are simply calculated from maximum and min-

Table 1
Periods of Completeness for Different Magnitude Intervals for the Two Seismic Catalogs (Same Instrumental Part (1962–1999) but Different Historical Magnitudes)*

Interval	3.5–4.4	4.5–4.9	5.0–5.4	5.5–5.9	6.0–6.4	6.5– . . .
Period S	1962–1999	1920–1999	1870–1999	1870–1999	1800–1999	1500–1999
Period L	1962–1999	1900–1999	1870–1999	1800–1999	1500–1999	1500–1999

*S, the catalog with Scotti magnitudes; L, the catalog with Levret magnitudes.

Table 2
Seismic Parameters for the 17 Selected Source Zones, Estimated with Weichert's Method (1980)

Zone	Nom	$\beta + \sigma(\beta)$	$\lambda + \sigma(\lambda)$	λ_{norm}	No. of events	Depth (km)
3	Mons-Aix la Chapelle	2.11 ± 0.32	0.48 ± 0.15	0.50	23	10
4	Fossé rhénan inférieur	2.01 ± 0.23	0.74 ± 0.15	0.36	35	10
6	Massif armoricain Nord	1.73 ± 0.19	1.12 ± 0.14	0.15	55	20
8	Fossé rhénan supérieur	1.33 ± 0.22	0.37 ± 0.13	0.19	22	10
10	Massif armoricain Sud	2.18 ± 0.12	3.24 ± 0.15	0.33	147	15
11	Limagnes	1.80 ± 0.34	0.28 ± 0.14	0.11	14	10
13	Jura	1.87 ± 0.32	0.46 ± 0.14	0.25	22	5
16	Pré-Alpes et pennique suisse	1.97 ± 0.20	1.27 ± 0.15	1.00	59	10
17	Région du Valais	1.66 ± 0.18	0.87 ± 0.14	1.48	45	10
18	MCE-Front pennique Nord	2.16 ± 0.37	0.47 ± 0.15	0.35	21	10
19	MCE-Front pennique Sud	1.58 ± 0.26	0.53 ± 0.14	1.34	27	10
20	Ivrea Sesia	1.84 ± 0.20	1.13 ± 0.14	1.44	54	15
23	Chaînes subalpines méridionales	1.98 ± 0.16	1.39 ± 0.15	0.98	66	10
27	Pyrénées Nord	3.09 ± 0.33	1.51 ± 0.16	0.95	61	10
30	Pyrénées Occidentales Nord	2.29 ± 0.12	4.13 ± 0.15	6.16	183	15
32	Pyrénées Orientales	2.21 ± 0.36	0.40 ± 0.15	0.36	18	10
37	Pyrénées Sud	2.35 ± 0.33	0.69 ± 0.15	0.67	30	10

β, slope of the Gutenberg–Richter; λ, the cumulative annual rate above magnitude 3.5; λ_{norm}, normalized to a 100 × 100 km^2 area.

imum latitude and longitude coordinates of the source zone apexes). As explained in the introduction, neither alternative zoning schemes nor alternative attenuation relationships are considered here. Following Beauval and Scotti (2003a,b), computations of seismicity parameters are based on the behavior of M 3.5 and above (see Table 1). These results deal with PGA; comparisons with results for spectral accelerations at three other frequencies (1, 2, and 5 Hz) are discussed at the end.

For all individual impacts, the same reference set of "conservative" parameter values is used: (1) seismic parameters are computed using the most conservative M-I correlation; (2) hazard computations are performed from minimum magnitude 3.5; (3) hazard computations are performed with no truncation of the lognormal distribution of ground motion, as done in the recent study for the revision of the French seismic zoning (Martin *et al.*, 2000a,b); and (4) finally, for simplicity in this impact study, maximum magnitude is fixed at 7.0 for all source zones to cover the greatest observed historical magnitudes. Maximum magnitudes estimates reach 7.0 in our catalogs, as well as in neighboring catalogs (e.g., the Bâle earthquake in the Earthquake Catalog of Switzerland [ECOS]). Maximum magnitude estimates greatly vary from one source zone to the other but they remain very difficult to assess. The impact (or variability) is measured as the difference between the reference hazard value and the newly computed one, changing one parameter at a time. Differences are normalized to reference hazard values and expressed as percentages. The reference set is always more conservative than the alternative one; impacts are thus positive normalized differences.

Modeling Uncertainties Due to Magnitude and Location Determination

All seismic catalogs are affected by uncertainties in both magnitude and location estimates. On the one hand, the historical intensities rely on interpreted written descriptions of the effects of earthquakes on people and buildings. On the other hand, the instrumental events often are attributed different magnitudes and locations, depending on the institution. To take these uncertainties into account, we first model catalog uncertainties for each seismic event and then use synthetic catalogs to study the impact of such uncertainties on hazard estimates.

Monte Carlo Simulations. The errors on magnitude and location determinations are modelled by three probability density functions (PDFs). Synthetic catalogs are generated through a Monte Carlo process; each event is assigned a new magnitude and new geographical coordinates selected from their PDF. A uniform distribution is attributed to historical magnitudes (see example in Fig. 2b). For an historical event, as explained in the data section, a magnitude is calculated for each intensity class with a M-I correlation; the minimum and the maximum magnitudes obtained are used as minimum and maximum thresholds for the uniform PDF. The width distribution for the uniform PDF shows that the average is approximately one magnitude unit (Fig. 2d). A Gaussian distribution centered on the original magnitude models the error on instrumental magnitude (example in Fig. 2a). The standard deviation is the error reported in the LDG instrumental catalog. Standard deviations are approximately 0.2 on average (Fig. 2b). The errors on latitude and longitude coordinates are also modeled by Gaussian distributions centered on the original values. The instrumental coordinates and the historical ones referenced with a location quality A in the SisFrance database (15% of selected historical events) are attributed a 5-km standard deviation. Attributed standard deviation is 10 km for historical locations of quality B events (25%), 20 km for quality C (22%), and 50 km for quality D (38%) events.

Generating N synthetic catalogs, the subcatalogs of the source zones are extracted N times, N sets of seismic parameters are obtained for each source zone, and N hazard values are calculated at each site. Figure 3 displays, as an example, the resulting Gutenberg–Richter curves for the Jura zone (gray curve) together with the corresponding distributions for both seismic parameters. Although we used $N = 200$, which is sufficiently large to obtain results with a representative variability, the variability is contained within one standard deviation of β, as calculated by Weichert's method on the original catalog (dashed black lines). Additional variability may have been obtained if completeness periods could have been automatically computed for each synthetic catalog.

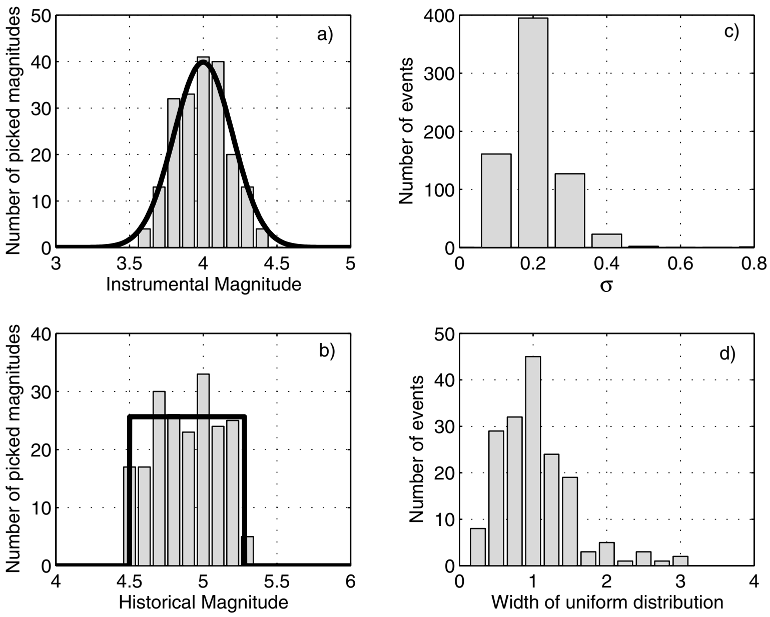

Figure 2. Example of 200 magnitudes selected from the PDF with a Monte Carlo approach (black curve) (a) Instrumental magnitude. PDF is centered on the original instrumental M 4.0 and with $\sigma = 0.2$. (b) Historical magnitude. PDF is a uniform distribution. (c) Distribution of the σ of the instrumental magnitudes used. (d) Distribution of the widths of the uniform PDF of the historical magnitudes used.

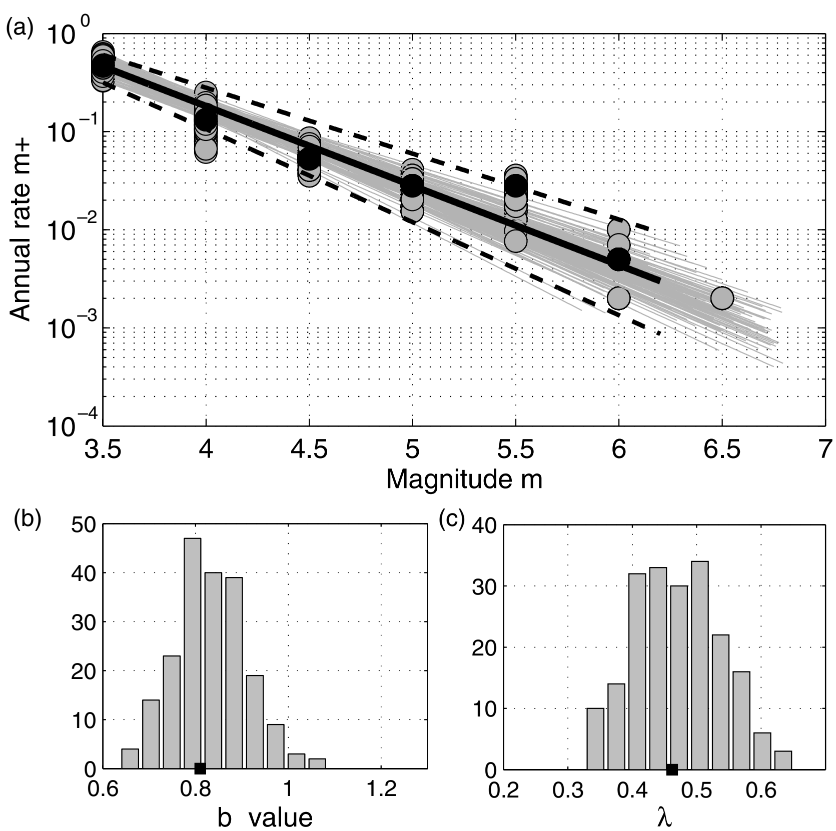

Figure 3. Distribution of seismic parameter values obtained with the Monte Carlo approach for the Jura source zone (zone 13). (a) Plain circles, observed annual rates; lines, recurrence curves; black refers to the original catalog (dashed lines take into account standard deviations of β and λ); gray refers to the 200 synthetic catalogs. (b) Distribution of the 200 b-values ($b = \beta/\ln 10$). (c) Distribution of the 200 seismic rates ($M \geq 3.5$).

Results. At each site, a distribution of 200 accelerations is obtained for each return period. The dispersion of the distribution, or the variability of hazard estimation due to catalog uncertainties, is quantified by calculating the coefficient of variation (COV, standard deviation of distribution divided by the mean and expressed as a percentage); the results are displayed in Figure 4. COVs vary between 2% and 17%, depending on the site and the return period. The COV is directly linked to the number of events used (see Table 2); the higher the number of events, the lower the coefficient of variation (the more stable the hazard results). Lowest COVs are obtained for sites in source zones 10 and 30 (≤5%), which contain the highest number of events. Furthermore, COV values increase with increasing return period (the increase is, however, small). This is because, for the same change in the *b*-value, the resulting difference in recurrence rates increases with magnitude. Uncertainties on magnitude and location determination of past events can hardly be reduced. Thus, the variability on hazard results due to catalog uncertainties is the minimum variability of any hazard calculation.

On the Choice of Magnitude-Intensity Correlation

Figure 5 shows the variability on hazard results due to a change in the M-I correlation, calculated for each site (dark-gray curves). Each curve corresponds to a different return period; the thicker the curve, the higher the return period. Accelerations are interpolated for return periods 100, 475, 10^3, 10^4, and 10^5 years. The impact of the choice of the M-I correlation ranges between 2% and 34%, depending on the site but does not significantly vary with the return period. Highest impacts are obtained for sites in zones 6, 11, and 19 (23%, 34%, and 24%). The explanation for the different impacts between sites appears clearly in Figure 6; impacts at 475 years are plotted as a function of the number of events in the instrumental magnitude bin 3.5–4.5 divided by the total number of events used. A high coefficient corresponds to a high proportion of small instrumental magnitudes. Seismic parameters of source zones 6, 11, and 19 are computed on subcatalogs containing, respectively, 57%, 59%, and 66% of their magnitudes between 3.5 and 4.5 and show a higher impact than that of source zones 4, 16, and 27 (smallest impacts, ≤9%), which are computed on subcatalogs containing, respectively, 80%, 80%, and 93% magnitudes between 3.5 and 4.5. This result is not surprising, because the choice of the M-I correlation only affects historical magnitudes and instrumental magnitudes higher than 4.5 are not numerous. Thus, in zones where seismicity models are controlled by a high number of instrumental events, the impact of a M-I correlation choice will be less important.

On the Choice of Truncating the PDF Distribution Modeling Ground-Motion Dispersion

A magnitude-distance couple may produce different ground motions; this dispersion is real and must be considered. In the Cornell–McGuire probabilistic method, this dispersion is taken into account when computing the probabilities of exceedance of target ground motions. The coefficients of the attenuation relationship used in this study are calculated by regression on the accelerograms of a database with 83% records coming from Europe and 17% from California (Berge-Thierry *et al.*, 2003). Thus, many sources, propagation paths, and site effects are mixed, leading to a great scatter ($\sigma_{\log_{10}A} = 0.2923$). Site effect classifications are rather crude and a precise description of the soil beneath the seismological stations is often not available. However, this description is often limited to 30 m and even if we had reliable V_S measurements over the upper 30 m at every single

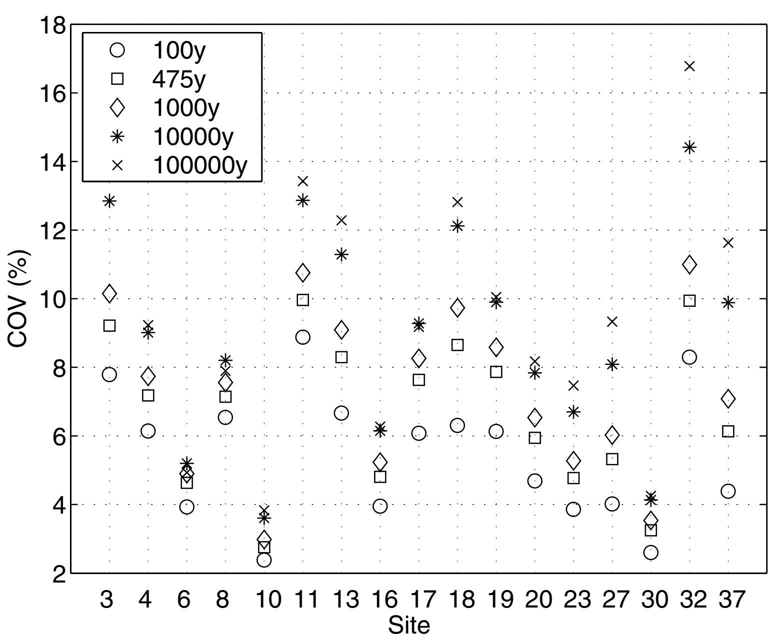

Figure 4. COVs (standard deviation divided by mean) of hazard estimations due to uncertainties on magnitude and location determinations. Hazard has been computed at the centers of the 17 source zones for five return periods.

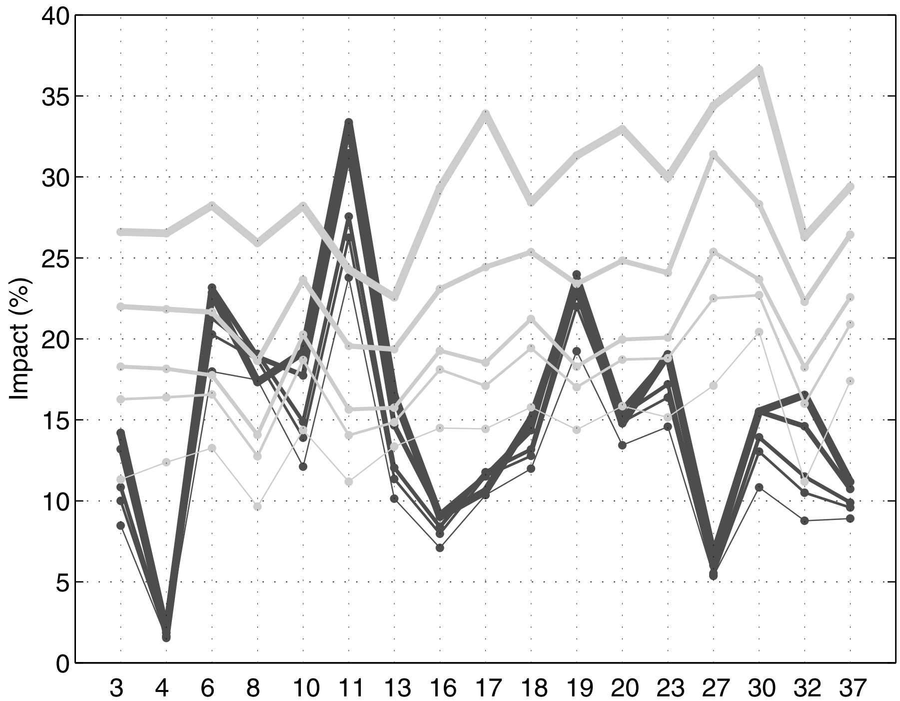

Figure 5. Impacts on hazard estimates of two parameters at the 17 sites. The thicker the line, the higher the return period (100, 475, 10^3, 10^4, and 10^5 years). Dark-gray points, impacts of the choice of the M-I correlation; light-gray points, impacts of the decision of truncating the predicted ground-motion distribution at $+2\sigma$.

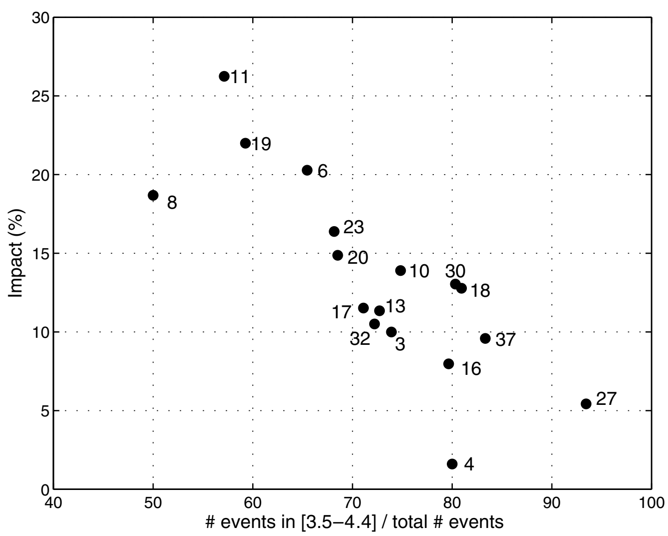

Figure 6. Impacts of the choice of the M-I correlation at 475 years at the 17 sites versus proportion of magnitudes [3.5–4.4] in the subcatalogs of the source zones.

recording station, the scatter would probably still be large because of the influence of the deeper geological structure on the nature of surface motions. Furthermore, in this attenuation relationship, the standard deviation is calculated as a function of frequency (variation is small) but not as a function of magnitude.

The current way of taking into account, in the hazard calculation, the dispersion on ground motion has strong drawbacks. As early as the beginning of the 1990s, Reiter's (1990) book on PSHA was evoking the consequences of the use of the lognormal distribution to compute probabilities of exceedance. Indeed, the very-low-likelihood accelerations in the tails of the distributions can significantly contribute to the seismic hazard estimations, when corresponding to high-likelihood magnitudes. The choice of the minimum magnitude thus can be of outmost importance. Some studies solve the problem by truncating the lognormal distribution, usually at a certain number of standard deviations above the mean (Abrahamson, 2000). In such cases, the accelerations with very small likelihood of occurrence can no longer contribute to the hazard. The result is a reduction of seismic hazard at all return periods. However, there is no physical reason why ground-motion upper bounds for all magnitude-distance couples should be at the same percentage above the median (Bommer, 2002). This way of truncating does not rely on any physical basis; consequently, there is no consensus on how much the lognormal distribution should be truncated. Reiter (1990) deals with truncations from 2.5σ to 4.5σ. Anderson and Brune (1999a) use a cutoff at 3σ. Abrahamson (2000) shows with statistical techniques that the data do not follow a lognormal distribution above 2σ and proposes a cutoff at 2 or 3σ; he clearly rejects truncation at 1σ, which would imply an underestimation of hazard. Based on the same observation, Restrepo-Velez and Bommer (2003) propose a modification of the upper tail of the distribution. The problem of truncating or not the attenuation relationship and how much is often not addressed in current PSHA studies, even in sensitivity studies. However, in a recent article, Bommer *et al.* (2004) discuss the consequences of the truncation and propose a framework for the determination of upper bounds on earthquake ground motions.

The impact of the decision to truncate the predictions of the attenuation relationship is here quantified by calculating the difference between no truncation and cutoff at $+2\sigma$. This truncation level corresponds to the 97.7-percentile and hence to a 1-in-50 chance of this level of ground motion to be exceeded. The Gaussian probability distribution is renormalized to unity after applying the truncation. The results are displayed in Figure 5 (light-gray curves). The higher the return period, the higher the impact of the PDF truncation, for all sites. Deciding to reject ground motions above 2σ produces a reduction in the hazard estimates of 10%–20% for a 100-year return period and of 23%–37% for 10^5 years. Impacts are quite stable from one site to the other. The contributions of the low-likelihood motions (the chance of exceeding 2σ is 2.3%) to hazard estimates are thus very important.

On the Choice of Minimum Magnitude (M_{min})

Once the seismic parameters are calculated, one has to decide the minimum magnitude that will contribute to the hazard. This magnitude is not linked to the magnitude range used to compute the Gutenberg–Richter parameters; it should be the minimum magnitude producing "significant" ground motions. Increasing M_{min} narrows the magnitude range contributing to the hazard; thus, the hazard may be reduced. It is often thought to be of small significance because it deals with events that are the least likely to produce significant ground motions. On the contrary, its impact on hazard estimations may be important due to the way of computing probabilities of exceedance. Small magnitudes can contribute largely, counterbalancing their small probabilities of exceeding the target level by their high annual rates. Although this problem was raised more than 10 years ago (Benjamin and Associates, 1989; Bender and Campbell, 1989; Reiter, 1990; Bender and Perkins, 1993), most PSHA studies do not even state the minimum magnitude used. However, following Bender and Perkins (1993), Grünthal and Wahlström (2001) showed that the choice of the minimum magnitude influences hazard results at small-return periods by superimposing hazard curves calculated with the minimum magnitudes 3.5, 4.0, and 4.5 for a single site in the lower Rhine embayment. Here, we quantify the impact of the choice of minimum magnitude at the 17 sites by comparing hazard levels for minimum magnitude 3.5 and 4.5. A minimum magnitude of 4.5 is used in all U.S. Geological Survey national seismic hazard maps (Frankel, 1995); whereas 3.5–4.0 is the magnitude range of minimum magnitudes used in the revision of the French zoning (Martin *et al.*, 2002a).

Results are displayed in Figure 7 (black curves). Again, the thicker the curve, the higher is the return period. As expected, the impact of the minimum magnitude on hazard results is decreasing with increasing return periods. Ground-motion thresholds increase with increasing return periods, and the contribution to the annual rates coming from small magnitudes decreases. Furthermore, the influence of M_{min} is highly site dependent. For 100 years, the impact can be very high, reaching 39% and 35% in zones 3 and 32. For the same return period, the lowest impacts ($\leq$10%) are found in the Alps, zones 17, 19, and 20. Beyond return period 10^3 years, the choice of a minimum magnitude between 3.5 and 4.5 does not influence the hazard anymore; for return periods 10^4 and 10^5 years, all impacts (except for zone 27) are between 0% and 5%.

The influence of M_{min} is in fact linked to the slope of the Gutenberg–Richter. Plotting the impacts versus the slopes of the Gutenberg–Richter reveals roughly a linear trend (Fig. 8). The sites with the higher β-value (or steeper recurrence slopes) show the higher sensitivity to the choice of a minimum magnitude. This trend is logical, as β represents the proportion of small and large magnitudes; high β implies a relatively higher proportion of small earthquakes than a low β. The Pyrenees zone 27 shows the highest impact at 10^4 and 10^5 years because the β-value of this zone is particularly high (3.1). The subcatalog of this zone indeed contains 93% of magnitudes in the interval 3.5–4.4 (Fig. 6). Moreover, the annual seismic rates (normalized to a 100×100 km^2 surface, Table 2) of each source zone are indicated by the color bar. For comparable slopes, the impact decreases with increasing seismic rate; thus, the choice of the minimum magnitude is more crucial in moderate seismic regions than in high seismic regions. The same tendency is obtained with the 100-year return period.

On the Choice of Maximum Magnitude (M_{max})

Contrary to the minimum magnitude, all sensitivity studies in PSHA address hazard variability due to the choice of the maximum magnitude. In contrast to the lower bound magnitude, maximum magnitude is zone specific and corresponds to the maximum magnitude that can occur inside a source zone. Estimating the maximum possible magnitude

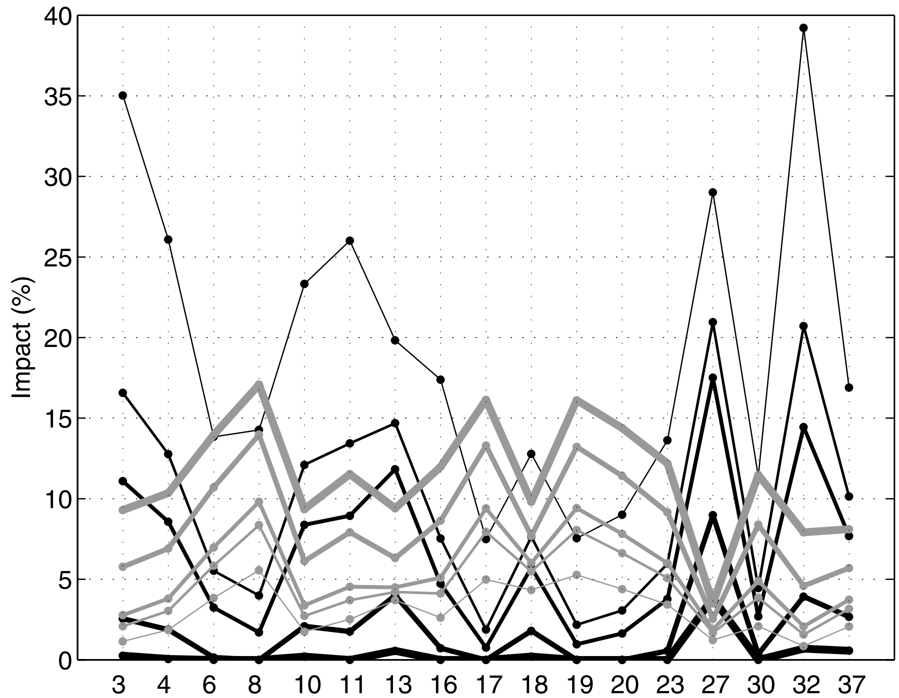

Figure 7. Impacts on hazard estimates for PGA of minimum and maximum magnitudes at the 17 sites. The thicker the line, the higher the return period (100, 475, 10^3, 10^4, and 10^5 years). Black points, impacts of the choice of M_{min} (3.5/4.5); gray points, impacts of the choice of M_{max} (6.5/7.0).

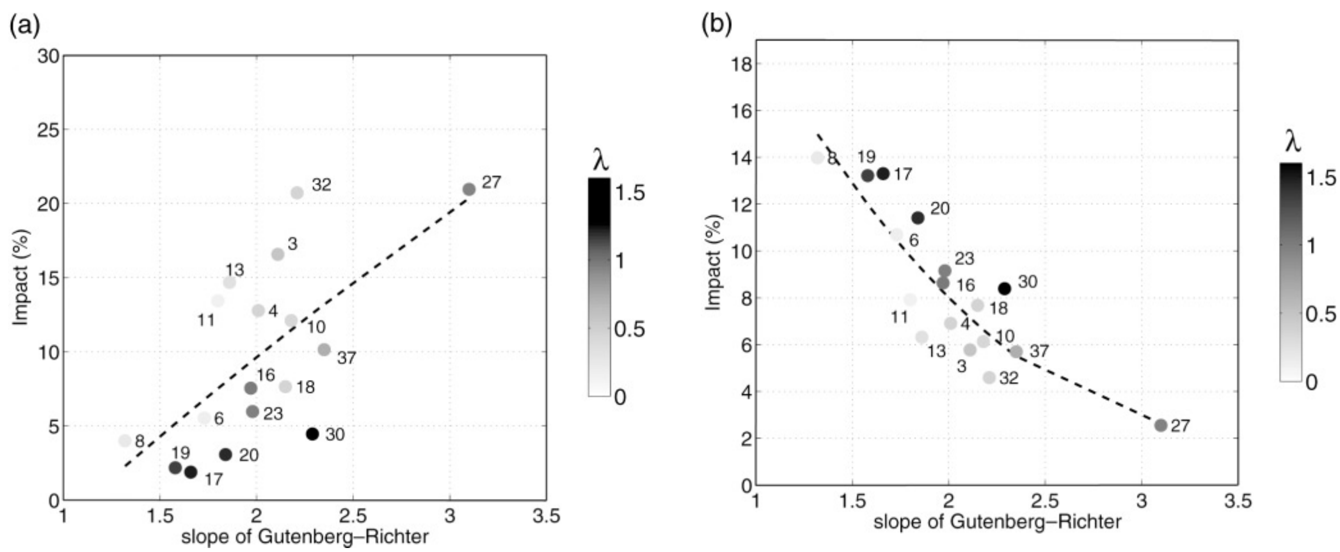

Figure 8. (a) Impacts of the choice of M_{min} at the 17 sites versus Gutenberg–Richter (GR) slopes of the source zones; hazards correspond to PGA at 475 years. (b) Impacts of the choice of M_{max} at the 17 sites versus GR slopes of the source zones; hazards correspond to 10^4 years. Note the scale difference. Colorbar, annual seismic rate of each source zone, normalized to a 100 × 100 km² surface.

in the seismotectonic source zones (using fault length or estimated slip and displacement of paleoseismic events) is difficult, since active faults are poorly known in an intraplate environment such as France. This maximum magnitude may not be linked to the magnitude range used to compute the Gutenberg–Richter parameters. In the reference data set, M_{max} is 7.0 for all zones, corresponding to the maximum magnitudes of the historical catalogs. The impact of M_{max} is estimated, decreasing M_{max} from 7.0 to 6.5. As shown previously (Fig. 2), uncertainties on historical magnitudes are large (0.5° on average if considering half-widths of uniform distributions). When changing the upper bound magnitude, we keep the cumulative seismicity rate of the minimum magnitude constant. Changing the upper bound magnitude has very little effect on the rates of smaller earthquakes because they are much more numerous.

The influence of maximum magnitude (Fig. 7, gray curves) shows a trend opposite to that of the minimum magnitude; with increasing return period, the influence of the maximum magnitude on hazard results increases. At small return periods ($\leq 10^3$ years), the variability due to the choice of the maximum magnitude stays smaller than 10%. Maximum influence is reached for return period 10^5 years in zones 8, 17, and 19 with 16%. The graph of Figure 8 shows the distribution of impacts versus the slopes of Gutenberg–Richter for the 10^4-year return period. The same tendency is obtained with the return period 10^5 years. The higher the slope, the lower the impact of the choice of $M_{\max}$, therefore opposite to the trend observed for the $M_{\min}$ impacts. When the slope of the Gutenberg–Richter increases, the proportion of high magnitudes versus small magnitudes decreases. Therefore, the contribution to the seismic hazard of the high-magnitude range [5.0 $M_{\max}$] decreases. Furthermore, contrary to the $M_{\min}$ impacts, for comparable slopes, impacts increase with increasing seismic rates. The choice of maximum magnitude is therefore more crucial in high seismic regions than in moderate seismic ones.

These calculations show the small contribution of the high-magnitude range to the estimation of hazard, even at very large return periods, in a moderate seismicity region such as France. Proper maximum magnitudes should be estimated for each zone based on geological, seismological, and geophysical features; however, this test quantifies the impact of maximum magnitude and shows that this parameter is not the controlling parameter in PSHA for France when considering PGA.

Radius of Influence of Hazard Estimates

The clear trends obtained between parameter impacts computed at the centers of the source zones and the seismic inputs of these zones indicate that hazard contributions come mainly from magnitude–distance couples inside the source zones, as shown in Figure 9 where for each site the maximum distance $D_{98\%}$ necessary to accumulate 98% of the contributions is computed at the 475- and 10^4-year return period.

Overall Variability

A logic tree can be constructed to compute the overall variability at each site; intermediate values in the parameter intervals explored in individual studies are selected and the hazard computation is performed for all possible combinations of parameters. Thus, explored minimum magnitudes are 3.5, 3.7, 3.9, 4.1, 4.3, and 4.5; the explored number of standard deviations for truncation are 2, 2.3, 2.7, 3.0, and ∞; and the explored maximum magnitudes are 6.5, 6.75, and 7.0. These intermediate values are necessary to get a smooth hazard distribution. Two M-I correlations are used; therefore, 180 hazard values are computed at each site. An example of such a distribution is displayed in Figure 10 for the site in zone 16. Results may be represented with mean, maximum, minimum, and percentiles, as shown in Figure 11. Furthermore, to each hazard value is associated a catalog uncer-

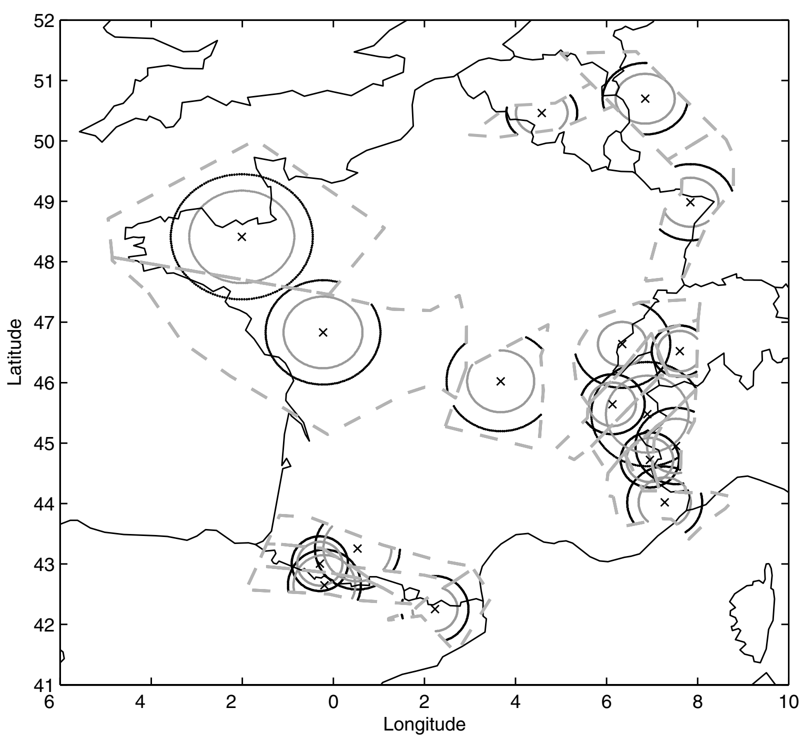

Figure 9. Maximum distance necessary at each site for reaching 98% of the hazard contributions, for the PGA and at return periods 475 years (black circles) and 10^4 years (gray circles).

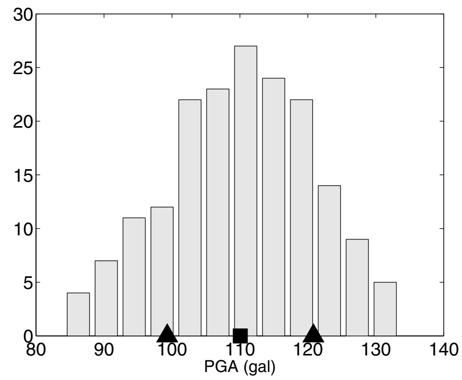

Figure 10. Distribution of 180 acceleration values for 100-year return period, resulting from the logic tree and computed at the center of source zone 16. Square and triangles, mean and standard deviations of distribution (1 gal = 1 cm·s^{-2}).

tainty (due to magnitude and location determination) calculated previously. The standard deviation characterizing catalog uncertainties is thus added to the minimum and maximum hazard values, at each return period, to get the full variability. Such a representation may be obtained at all sites and enables the estimation of the range of possible PGA values for any return period between 100 and 10^5 years. To quantify the overall variability, the COV is calculated for each site at the five return periods; values vary mainly between 10% and 20%.

Impacts as a Function of Frequency

The results presented so far deal with the acceleration at PGA. We have performed the same computations for frequencies 1, 2, and 5 Hz. At 5 Hz, the impacts and their hierarchy are very similar to results at the PGA. At 2 Hz, however, important differences appear that increase at 1 Hz; while minimum magnitude does not play a role anymore whatever the return period, impacts of correlation and truncation increase significantly. But above all, the impact of maximum magnitude increases, reaching the level of both correlation and truncation impacts at 10^4 years. Individual impacts of minimum and maximum magnitudes, at the five considered return periods, are displayed in Figure 12 for frequency 1 Hz. The understanding of the changes in maximum magnitude impacts between the PGA and 1 Hz is straightforward when performing magnitude deaggregation; Figure 13a,b shows distributions of contributions in magnitude for both frequencies at one example site. At the PGA, contributions come from the whole range of magnitudes, whereas at 1 Hz contributions mainly come from the upper range of magnitudes. Deaggregation in distance (Fig. 13c,d) indicates that contributions at 1 Hz come from larger distances than at PGA. Furthermore, Figure 14 displays the logic tree results for the return period 10^4 years at the four considered frequencies. Values corresponding to frequencies 2, 5, and 34 Hz (PGA) are multiplied by a coefficient so that the mean value of each distribution equals the mean value of distribution at 1 Hz (see the legend to Fig. 14). Percentages correspond to differences between maximum and minimum values, normalized by the maximum value. As expected from individual impact studies, variability increases with decreasing frequencies (40% at PGA and 60% at 1 Hz).

Discussion and Conclusions

The hierarchy of the impacts of the four parameters changes from one site to the next, but global tendencies can be drawn (Fig. 15). Results at 475 years represent small re-

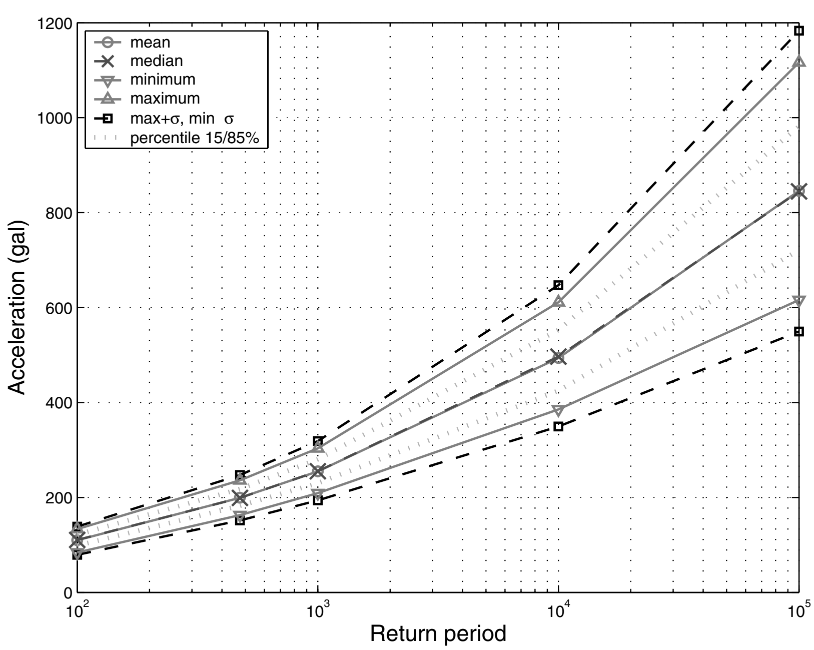

Figure 11. Results of the logic tree, considering all possible combinations of the four parameters at the center of source zone 16. Computations have been performed for the five return periods: 10^2, 475, 10^3, 10^4, and 10^5 years. Standard deviation σ due to catalog uncertainties is added to both minimum and maximum hazard values (1 gal = 1 cm·s^{-2}). Notice that mean and median are very similar.

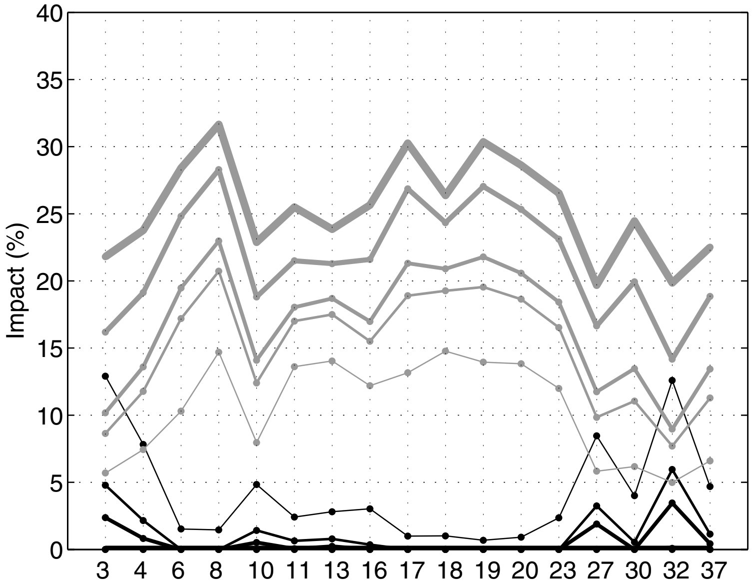

Figure 12. Impacts on hazard estimates of M_{min} and M_{max} for frequency 1 Hz at the 17 sites. The thicker the line, the higher the return period (100, 475, 1000, 10^4, and 10^5 years). Black points, impacts of the choice of M_{min} (3.5/4.5); gray points, impacts of the choice of M_{max} (6.5/7.0).

turn periods ($<10^3$ years), whereas results at 10^4 years represent large return periods ($>10^3$ years). Catalog uncertainties are also superimposed on the impacts of the other four parameters shown in Figure 15. The variability of catalog uncertainty is here quantified through the coefficient $[2\sigma/(\mu + \sigma)]$, with σ and μ being the standard deviation and mean of the Gaussian distribution, respectively.

The following main conclusions can be drawn:

- Catalog uncertainties that underlie all hazard results can engender variability as high as the variability caused by the controlling parameters.
- The minimum magnitude can greatly influence the estimation of hazard at small return periods; however, hazard estimations at large return periods or at low frequencies are not affected by this choice.
- The choices of an M-I correlation and of the truncation of the predicted ground-motion distribution are key parameters in hazard estimation at all return periods and their impact increases with decreasing frequency.
- The choice of the maximum magnitude has a relatively small impact on PGA hazard estimations, even for very large return periods, but it becomes a key parameter at lower frequencies (<5 Hz).

The conclusions dealing with the impact of minimum and maximum magnitudes are what would be intuitively expected; the value of this study lies in quantifying the sensitivities. Given such a hierarchy of impacts, clearly, PSHA studies for France should carefully select values for these parameters in order to minimize biases in the calculations. Hazard should be computed from a minimum magnitude of 4.0 (in the nuclear safety community, a minimum magnitude of 5.0 is usually used). The database from which the Berge-Thierry *et al.* (2003) attenuation relationship is derived, for example, does not contain events with magnitudes lower than 4.0. Using this relationship to predict ground motions of magnitudes 3.5–3.9 implies extrapolating the relationship. No consensus exists on how much the probability functions predicted by the attenuation relationship should be truncated. Hazard should therefore be estimated by testing several trun-

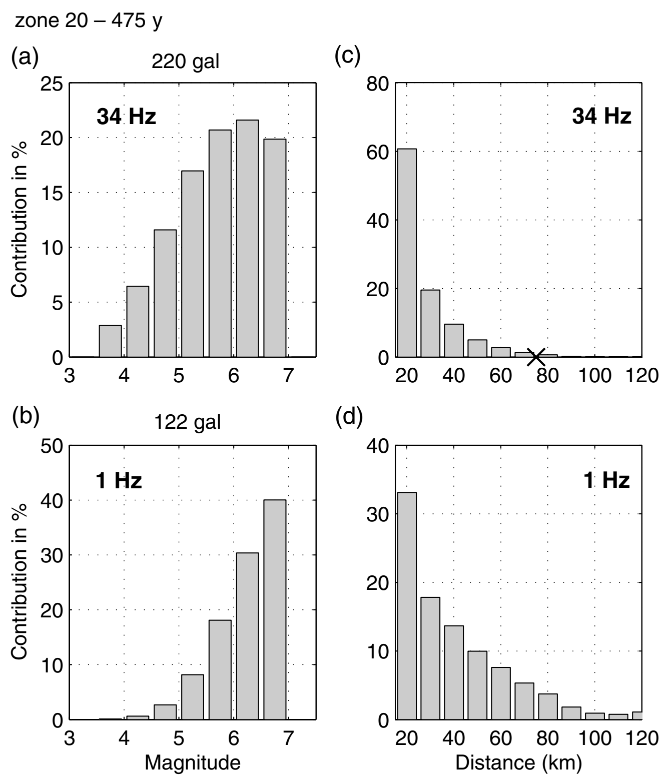

Figure 13. Deaggregation for two different frequencies (PGA and 1 Hz), for 475-year return period and site 20. (a, b) Magnitude distribution of contributions and (c, d) distance distribution of contributions. Cross corresponds to $D_{98\%}$.

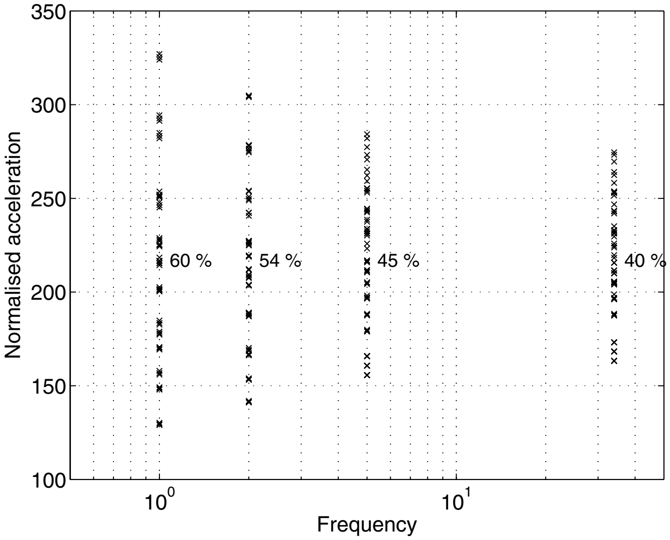

Figure 14. Accelerations calculated at frequencies 1, 2, 5, and 34 Hz (PGA), for a 10^4-year return period, exploring all parameter combinations of the logic tree at the center of zone 30. For each distribution at frequencies 2, 5, and 34 Hz, values have been multiplied by the coefficient: m_i/m_1, with, respectively, m_i and m_1 the means of distributions at frequencies i and 1 Hz. Percentages quantify variability (difference between minimum and maximum values divided by maximum value).

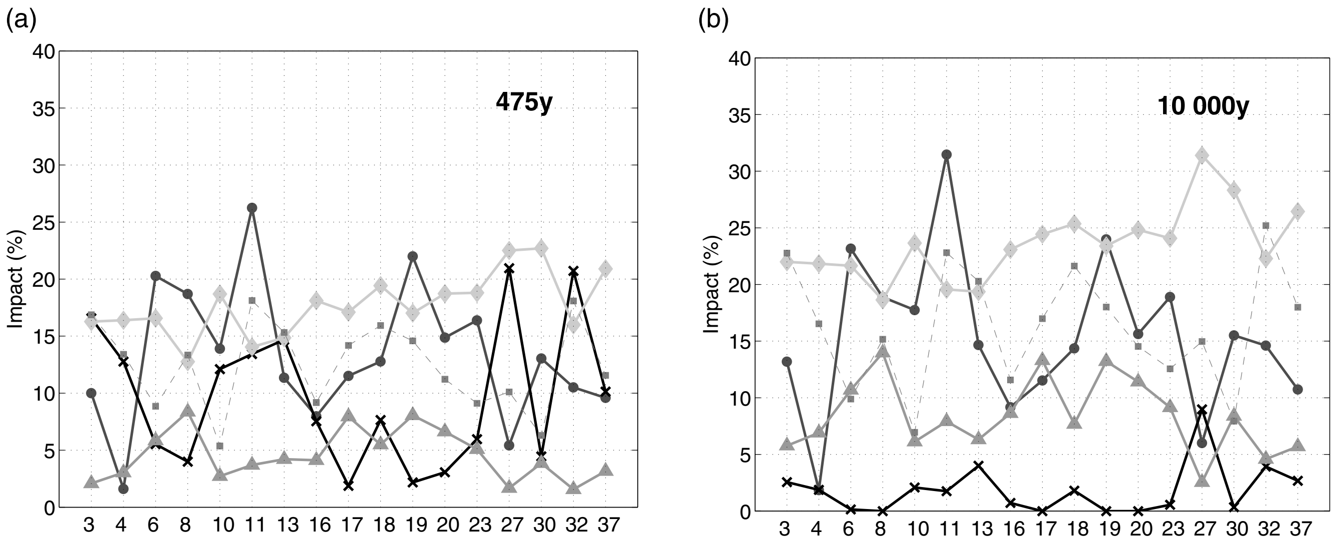

Figure 15. Comparisons of individual parameter impacts at 475-year (a) and 10^4 year (b) return periods, at the 17 sites and for PGA. Points, M-I correlation impact; diamonds, truncation; crosses, M_{min}; triangles, M_{max}. Variabilities due to catalog uncertainties are superimposed (squares).

cation levels, until physical models are proposed that may allow the estimation of upper bounds to ground motions (see Restrepo-Velez and Bommer [2003] and Bommer *et al.* [2004]). Bakun and Scotti (unpublished manuscript) are currently working on improving the M-I correlation by considering the regional intensity attenuation relationship for the French metropolitan territory. Results from this work will hopefully reduce the M-I conversion uncertainty. Finally, results show that reductions of maximum magnitudes from values of 7.0 to 6.5 produces reductions in the hazard estimates that are less than half the reductions due to the decision of truncating the predicted ground-motion distribution at two standard deviations. This holds at all return periods and frequencies down to 5 Hz. However, these results cannot be generalized for lower frequencies where the estimation of maximum magnitudes becomes as important as the decision of truncating the attenuation relationship. Geological considerations accompanied by statistical studies on seismic catalogs (for example, Pisarenko *et al.* [1996]) become important to specify the upper bound of the magnitude range. The overall variability in hazard estimates due to these four parameter choices (COV between 10% and 20% at PGA) shows that better physical models are needed before reliable PSHA estimates may be obtained. Seismotectonic zones are a very crude representation of "source" zones, attenuation models are all weakly constrained in the near-source regions, and their predicted dispersions may be wrongly overestimated (Anderson and Brune, 1999b). Furthermore, if quantifications of impacts at each site can approximately be extrapolated to the whole zone, this study does not give any estimation of uncertainties on hazard outside the source zones. In these regions with weak seismic rate where large earthquakes may have occurred in the past (e.g., the Lambesc earthquake in the south–east part of France, *M* 6.0, Baroux *et al.* [2003]), the uncertainty on hazard estimates is very large and a completely different study should be carried out for its quantification.

Acknowledgments

This work would not have been possible without the cooperation of D. Bertil, L. F. Bonilla, and C. Clément. Many thanks go to Mario Ordaz for providing us with the source code CRISIS2000. We also thank all the colleagues of the BERSSIN laboratory for extensive and stimulating discussions; and finally, we thank J. J. Bommer for a thorough review that greatly improved the manuscript.

References

Abrahamson, N. A. (2000). State of the practice of seismic hazard evaluation, in *GeoEng 2000 Conference*, Australia, 19–24 November 2000.

Aki, K. (1965). Maximum likelihood estimate of b in the formula logN = a-bM and its confidence limits, *Bull. Earthquake Res. Inst.* **43,** 237–239.

Ambraseys, N. N. (1995). The prediction of peak ground acceleration in Europe, *Earthquake Eng. Struct. Dyn.* **24,** 467–490.

Ambraseys, N. N., K. A. Simpson, and J. J. Bommer (1996). Prediction of horizontal response spectra in europe, *Earthquake Eng. Struct. Dyn.* **25,** 371–400.

Anderson, J. G., and J. N. Brune (1999a). Methodology for using rocks in Nevada to test seismic hazard models, *Bull. Seism. Soc. Am.* **89,** no. 2, 456–467.

Anderson, J. G., and J. N. Brune (1999b). Probabilistic seismic hazard analysis without the ergodic assumption, *Seism. Res. Lett.* **70,** no. 1, 19–28.

Autran, A., J. L. Blès, Ph. Combes, M. Cushing, P. Dominique, C. Durouchoux, J. C. Gariel, X. Goula, B. Mohammadioun, and M. Terrier (1998). Probabilistic seismic hazard assessment in France. Part One: seismotectonic zonation, in *Proceedings of the 11th ECEE*, Paris, France, 6–11 September 1998.

Baroux, E., N. A. Pino, G. Valensise, O. Scotti, and M. E. Cushing (2003). Source parameters of the 11 June 1909, Lambesc (Provence, southeastern France) earthquake: a reappraisal based on macroseismic, seismological, and geodetic observations, *J. Geophys. Res.* **108,** no. 9, 2454, doi 10.1029/2002JB002348.

Beauval, C. (2003). Analyse des incertitudes dans une estimation probabiliste de l'aléa sismique, exemple de la France, *Ph.D. thesis*, University Joseph Fourier, France.

Beauval, C., and O. Scotti (2003a). Mapping b-values in France using two different magnitude ranges: possible non power-law behavior, *Geophys. Res. Lett.* **30,** no. 17, 1892, doi 10.1029/2003GL017576.

Beauval, C., and O. Scotti (2003b). Variabilité dans la modélisation de la récurrence des séismes et impact sur l'évaluation de l'aléa sismique en France, *6ème Colloque National AFPS*, Ecole Polytechnique, Palaiseau, 1–3 July 2003.

Bender, B., and K. W. Campbell (1989). A note on the selection of minimum magnitude for use in seismic hazard analysis, *Bull. Seism. Soc. Am.* **79,** 199–204.

Bender, B. K., and D. M. Perkins (1993). Treatment of parameter uncertainty and variability for a single seismic hazard map, *Earthquake Spectra* **9,** no. 2, 165–194.

Benjamin, J. R., and Associates (1989). Proceedings: engineering characterization of small-magnitude earthquakes, Electric Power Research Institute, EPRI-NP-6389.

Berge-Thierry, C., F. Cotton, O. Scotti, D. A. Griot-Pommera, and Y. Fukushima (2003). New empirical response spectral attenuation laws for moderate European earthquakes, *J. Earthquake Eng.* **7,** no. 2, 193–222.

Bommer, J. J. (2002). Deterministic vs. probabilistic seismic hazard assessment: an exaggerated and obstructive dichotomy, *J. Earthquake Eng.* **6,** 43–73.

Bommer, J. J., N. A. Abrahamson, F. O. Strasser, A. Pecker, P. Y. Bard, H. Bungum, F. Cotton, D. Faeh, F. Sabetta, F. Scherbaum, and J. Studer (2004). The challenge of defining upper bounds on earthquake ground motions, *Seism. Res. Lett.* **75,** no. 1, 82–95.

Cornell, C. A. (1968). Engineering seismic risk analysis, *Bull. Seism. Soc. Am.* **58,** no. 1, 1583–1606.

Dominique, P., A. Autran, J. L. Blès, D. Fitzenz, F. Samarcq, M. Terrier, M. Cushing, J. C. Gariel, B. Mohammadioun, Ph. Combes, C. Durouchoux, and X. Goula (1998). Part two: probabilistic approach, seismic hazard map on the national territory (France), *Proceedings of the 11th ECEE*, Paris, France, 6–11 September 1998.

Douglas, J. (2003). Earthquake ground-motion estimation using strong-motion records: a review of equations for the estimation of peak acceleration and response spectral ordinates, *Earth Sci. Rev.* **61,** 43–104.

Frankel, A. (1995). Mapping seismic hazard in the Central and Eastern United States, *Seism. Res. Lett.* **66,** no. 4, 8–21.

Giner, J. J., S. Molina, and P. Jauregui (2002). Advantages of using sensitivity analysis in seismic hazard assessment: a case study of sites in southern and eastern Spain, *Bull. Seism. Soc. Am.* **92,** no. 2, 543–554.

Griot-Pommera, D. A., and O. Scotti (2001). Estimating earthquake location and magnitude from French seismic intensity observations, *European Geophysical Society, XXVI General Assembly*, Nice, France, 25–30 March 2001.

Grünthal, G., and R. Wahlström (2001). Sensitivity of parameters for probabilistic seismic hazard analysis using a logic tree approach, *J. Earthquake Eng.* **5,** no. 3, 309–328.

Kramer, S. L. (1996). *Geotechnical Earthquake Engineering*, *Civil Engineering and Engineering Mechanics*, Prentice Hall, Upper Saddle River, New Jersey.

Levret, A., J. C. Backe, and M. Cushing (1994). Atlas of macroseismic maps for French earthquakes with their principal characteristics, *Natural Hazards* **10,** 19–46.

Martin, Ch., Ph. Combes, R. Secanell, G. Lignon, D. Carbon, A. Fioravanti, and B. Grellet (2002a). Révision du zonage sismique de la France, Etude probabiliste, Rapport GEOTER GTR/MATE/0701-150.

Martin, Ch., R. Secanell, Ph. Combes, and G. Lignon (2002b). Preliminary probabilistic seismic hazard assessment of France, in *Proceedings of the 12th ECEE*, London, England, 10–14 September 2002, Paper Reference 870.

McGuire, R. K. (1976). Fortran computer program for seismic risk analysis, *U.S. Geol. Survey Open-File Report 76-67*.

Mohammadioun, B., and A. Pecker (1993). Prévision du mouvement sismique au rocher à partir des données de mouvements forts actuellement disponibles, in *Proceedings 3e Colloque National AFPS "Génie parasismique et aspects vibratoires dans le génie civil,"* St. Rémy-Lès-Chevreuse, France, 24–26 March 1993.

Nicolas, M., N. Bethoux, and B. Madeddu (1998). Instrumental seismicity of the Western Alps: a revised catalogue, *Pageoph* **152,** 707–731.

Page, R. (1968). Aftershocks and microaftershocks, *Bull. Seism. Soc. Am.* **58,** 1131–1168.

Pisarenko, V. F., A. A. Lyubushin, V. B. Lysenko, and T. V. Golubeva, 1996. Statistical estimation of seismic hazard parameters: maximum possible magnitude and related parameters, *Bull. Seism. Soc. Am.* **86,** no. 3, 691–700.

Rebez, A., and D. Slejko (2000). Sensitivity analysis on the input parameters in probabilistic seismic hazard assessment, *Soil Dyn. Earthquake Eng.* **20,** 341–351.

Reiter, L. (1990). *Earthquake Hazard Analysis: Issues and Insights,* Columbia University Press, New York.

Restrepo-Velez, L. F., and J. J. Bommer (2003). An exploration of the nature of the scatter in ground-motion prediction equations and the implications for seismic hazard assessment, *J. Earthquake Eng.* **7,** 171–199.

Stepp, J. C. (1972). Analysis of completeness of the earthquake sample in the Puget Sound area and its effect on statistical estimates of earthquake hazard, in *Proc. Microzonation Conf.*, Seattle, Washington, 897–909.

Tento, A., L. Franceschina, and A. Marcellini (1992). Expected ground motion evaluation for Italian sites, in *Proceedings 10th World Conf. on Earthquake Engineering*, Madrid, Spain, 19–24 July 1992, Vol. 1, 489–494.

Utsu, T. (1966). A statistical significance test of the difference in b-value between two earthquake groups, *J. Phys. Earth* **14,** 37–40.

Weichert, D. H. (1980). Estimation of the earthquake recurrence parameters for unequal observation periods for different magnitudes, *Bull. Seism. Soc. Am.* **70,** no. 4, 1337–1346.

Institut de Radioprotection et de Sûreté Nucléaire
Bureau d'Evaluation des Risques Sismiques pour la Sûreté des Installations
BP 17
92262 Fontenay-aux-Roses Cedex
France

Manuscript received 8 December 2003.